Analysis of the singlet-triplet model for the copper oxide plane within the paramagnetic state

R. Hayn
Max-Planck-Institut für Festkörperforschung, D-7000 Stuttgart 80, Federal Republic of Germany

V. Yushankhai
Joint Institute for Nuclear Research, Head Post Office, P.O. Box 79, Moscow, Russia

S. Lovtsov
Irkutsk University, Faculty of Physics, 664003 Irkutsk, Russia

(Received 21 February 1992; revised manuscript received 2 December 1992)

The two-band Emery model has been reduced to an effective singlet-triplet model to describe the low-energy electronic properties of the CuO_2 plane in oxide superconductors. The effective Hamiltonian is written in terms of Hubbard operators, projecting onto local singlet and triplet states of a doped hole. The projection method for two-time Green's functions (GF's) is applied to obtain the band structure and the density of states in the paramagnetic state. It is found that a singlet band that is mainly of oxygen character is located between the antibonding copper and the nonbonding oxygen bands. The triplet part in the singlet band has been found to be very small. This is due to the small mixing parameter and because the local singlet-triplet transition is forbidden due to time-reversal symmetry. The results are in good agreement with a random-phase-approximation-like decoupling for the GF's of the original problem including the singlet operator [R. Hayn, Z. Phys. B **85**, 169 (1991)]. With doping, a transfer of spectral weight occurs from the copper and the triplet to the singlet band.

I. INTRODUCTION

One important problem concerning the normal-state electronic structure of the high-temperature superconductors is the reduction of the complex problem to a relatively simple, effective Hamiltonian that describes correctly all the low-lying excitations. An important step into that direction has been done by Zhang and Rice[1] who reduced the Emery model[2] of the copper oxide plane to an effective t-J model. For that purpose they used the local singlet state of a doped oxygen hole. Unfortunately, this reduction procedure raised some controversy.[3–6] For instance, the neglect of local triplet states, whose effects are of the same order in the small parameter t/Δ, was criticized. Here $\Delta = \varepsilon_p - \varepsilon_d$ is the difference between the oxygen (ε_p) and the copper (ε_d) atomic energies, and t is the hybridization between neighboring copper and oxygen orbitals. Further, it is even very questionable if this spin fluctuation regime $\Delta \gg t$ is realized in the considered materials.

To overcome the above-mentioned objections, two of the present authors[7] extended the reduction procedure of Zhang and Rice to the charge fluctuation region, which deals with much smaller values of Δ than the original work. Moreover, they included the triplet states and derived an effective singlet-triplet model. In the present paper we want to continue the analysis until we reach quantitative results for the band structure and the density of states of the copper oxide plane. Independently from our paper, the same "cell perturbation method" was used by Jefferson, Eskes, and Feiner[8] for an elaborate derivation of the single-band t-J model. Unlike our work, they calculated the effects of the triplet states only perturbatively. But the singlet-triplet model gives a much more complete picture of the electronic structure. This will be shown in the following for the density of states. The main purpose of the present work is the development of a technique to deal with such complicated Hamiltonians as the singlet-triplet model.

Several quite unexpected details of the electronic structure of the copper oxides have been revealed experimentally.[9,10] Particularly, it was found that with increasing hole doping, oxygen states in the charge-transfer gap between the antibonding copper and the nonbonding oxygen states are filled up with holes. The nature of these "midgap states" is still an open question. There are some attempts to explain such states within strongly correlated models. For example, such states have been found due to the scattering of holes at spin fluctuations[11] or with the help of the projection method starting from the antiferromagnetic ground state[12] and by a random-phase-approximation (RPA) -like decoupling of the equations of motion for Green's functions (GF's).[13] In our opinion the peculiarities of the band structure mentioned above, are closely connected with the singlet state of Zhang and Rice.[1] To make this point more clear, we present here numerical results of the electronic structure, including the singlet band, which show good agreement with our former RPA procedure,[13] which deals directly with the Emery model.

First we repeat shortly the derivation of the singlet-triplet model in a more transparent notation in Sec. II.

The model contains two different kinds of degrees of freedom: The local singlet or triplet states, which can be occupied by doped oxygen holes, and the localized spins associated with copper holes, which are already present in the undoped compound. In an attempt to treat the band structure of the doped CuO_2 plane with no long-range order of localized spins, we assume a classical paramagnetic ground state and neglect any antiferromagnetic short-range spin correlation.

In Sec. IV we derive the equations of motion for the singlet and triplet GF's. To take care of the difficult commutation relations of Hubbard operators in which the effective problem is written down, we employ here a projection technique for two-time Green's functions.[14] This is much better than the approximation of Hubbard operators by Fermi operators as in Ref. 6, where the influence of the singlet-triplet mixing has also been considered. To derive the equations of motion it is helpful to consider the time-reversal symmetry of the problem (Sec. III), which is also one reason for the relatively small effect of the singlet-triplet coupling. Finally, in Sec. V we present the numerical results.

II. DERIVATION OF THE SINGLET-TRIPLET MODEL

The idea of reducing the original Emery model[2] to an effective singlet-triplet problem is a very general one. We divide the original problem into small clusters, which will be diagonalized, but only the most important low-energy states will be incorporated into the relevant subspace. The hopping Hamiltonian between the clusters will be considered as a perturbation and the irrelevant subspace will be projected out. This has been done up to second order in the effective hopping parameter in Ref. 7. Now, we will repeat this procedure in a slightly changed, more transparent notation. We will restrict ourselves here to first order because we are not interested in the magnetic structure of the CuO_2 plane. In the following we briefly derive the most important formulas, which will be needed in the numerical analysis.

A. Starting Hamiltonian

Let us begin with the Emery model in its minimal version

$$H = -\Delta \sum_{i,\sigma} d^\dagger_{i\sigma} d_{i\sigma} + t \sum_{i,m,\sigma} S_{im} (d^\dagger_{i\sigma} p_{m\sigma} + \text{H.c.}) + U \sum_i d^\dagger_{i\uparrow} d_{i\uparrow} d^\dagger_{i\downarrow} d_{i\downarrow} \ , \tag{1}$$

where $d^\dagger_{i\sigma}$ and $p^\dagger_{m\sigma}$ denote the creation of a copper or oxygen hole, respectively. The signs $S_{im} = \pm 1$ have been chosen in agreement with Ref. 1, and the energy of the oxygen level ε_p will be our energy zero. Now we will bring the Hamiltonian (1) in a more convenient form to start with our procedure. First of all, we will project out doubly occupied copper states because the Hubbard U is the largest energy in the system. Furthermore we consider in the following only the symmetric combination of oxygen states:

$$p^{(s)}_{i\sigma} = \frac{1}{2} \sum_m S_{im} p_{m\sigma} \ . \tag{2}$$

There is yet an antisymmetric combination, which does not couple to the copper system and gives rise to a dispersionless nonbonding oxygen band at energy zero. We mention this nonbonding band only in the final results. So we obtain from (1)

$$H = -\Delta \sum_{i,\sigma} X^{\sigma\sigma}_i + 2t \sum_{i,\sigma} (X^{\sigma 0}_i p^{(s)}_{i\sigma} + \text{H.c.}) + \frac{4t^2}{U-\Delta} \sum_{i,\sigma} (X^{\sigma\bar\sigma}_i p^{(s)\dagger}_{i\bar\sigma} p^{(s)}_{i\sigma} - X^{\bar\sigma\bar\sigma}_i p^{(s)\dagger}_{i\sigma} p^{(s)}_{i\sigma}) \tag{3}$$

with $\bar\sigma \equiv -\sigma$ and where we used Hubbard operators,

$$X^{\sigma\sigma}_i = n_{i\sigma}(1 - n_{i\bar\sigma}), \quad X^{\sigma\bar\sigma}_i = d^\dagger_{i\sigma} d_{i\bar\sigma} \ , \qquad X^{\sigma 0}_i = d^\dagger_{i\sigma}(1 - n_{i\bar\sigma}) \tag{4}$$

with $n_{i\sigma} = d^\dagger_{i\sigma} d_{i\sigma}$.

The symmetrized oxygen operators (2) are not orthogonal. It is more convenient to go over to orthogonal Wannier operators $c_{j\sigma}$ in the familiar way:

$$p^{(s)}_{l\sigma} = \sum_j \lambda_{lj} \, c_{j\sigma}, \quad \lambda_{lj} = \frac{1}{N} \sum_k \frac{1}{2} \, \tilde\gamma_k \, e^{ik(l-j)} \tag{5}$$

with

$$\tilde\gamma_k = 2\sqrt{\sin^2(k_x/2) + \sin^2(k_y/2)} \ ,$$

where N is the number of copper atoms and the distance between neighboring Cu atoms has been chosen to be one. After the replacement of $p^{(s)}_{i\sigma}$ in (3) by the orthogonal Wannier states $c_{j\sigma}$ one can see that there exist corresponding hopping parameters $\sim \lambda_{lj}$ at any distance. But, in fact, the hopping parameters are rapidly decreasing functions of the distance $(l-j)$.[7] In the numerical calculations we will take into account only

$$\lambda_0 = \lambda_{ii} = 0.96 \ ,$$
$$\lambda_1 = -0.14 \quad \text{for } (i-j) = \pm \mathbf{a}_x \text{ or } \pm \mathbf{a}_y \ ,$$
$$\lambda_2 = -0.02 \quad \text{for } (i-j) = \pm(\mathbf{a}_x + \mathbf{a}_y) \text{ or } \pm(\mathbf{a}_x - \mathbf{a}_y) \ .$$

This restriction will be confirmed by additional arguments in Sec. IV C. In the new variables, the Hamiltonian will be divided into a diagonal part $H^{(i)}_0$ and a nondiagonal one $H^{(i,j)}_{\text{int}}$. After substitution of (5) into (3) and neglecting three center terms we obtain

$$H = \sum_i H^{(i)}_0 + \sum_{i,j}^{i \neq j} H^{(i,j)}_{\text{int}} \tag{6}$$

with

$$H^{(i)}_0 = -\Delta \sum_\sigma X^{\sigma\sigma}_i + V_0 \sum_\sigma (X^{\sigma 0}_i c_{i\sigma} + \text{H.c.}) + J \sum_\sigma (X^{\sigma\bar\sigma}_i c^\dagger_{i\bar\sigma} c_{i\sigma} - X^{\bar\sigma\bar\sigma}_i c^\dagger_{i\sigma} c_{i\sigma}) \tag{7}$$

and

$$H_{\rm int}^{(i,j)} = V_{ij} \sum_{\sigma} [X_i^{\sigma 0} c_{j\sigma} + \gamma (X_i^{\sigma\bar{\sigma}} c_{i\bar{\sigma}}^{\dagger} c_{j\sigma} - X_i^{\bar{\sigma}\bar{\sigma}} c_{i\sigma}^{\dagger} c_{j\sigma}) + \text{H.c.}] \tag{8}$$

with $V_{ij} = 2t\lambda_{ij}$, $V_0 = 2t\lambda_0$ and where the abbreviations

$$J = \frac{V_0^2}{U-\Delta}, \quad \gamma = \frac{V_0}{U-\Delta} \tag{9}$$

have been used. In the following we will diagonalize (7), and we will consider the hopping term (8) as a perturbation. This leads to the small parameter $V_1 = 2t\lambda_1$, which is more appropriate as expansion parameter than the hopping t of the original work.[1]

B. Diagonalization within one elementary cell

Fortunately, the diagonal part of the Hamiltonian (7) can be simply diagonalized, distinguishing between states with one or with two holes per site. For one hole one finds two degenerated ground states of mainly copper character for every spin σ (site index is dropped):

$$|f_\sigma\rangle = \cos\theta_1 \; d_\sigma^{\dagger}|0\rangle - \sin\theta_1 \; c_\sigma^{\dagger}|0\rangle \; , \qquad \tan 2\theta_1 = \frac{2V_0}{\Delta} \tag{10}$$

with the energy

$$E_f = -\frac{\Delta}{2} - \sqrt{\frac{\Delta^2}{4} + V_0^2} \; . \tag{11}$$

The one hole states with mainly oxygen character have an energy of the order Δ higher than E_f and are projected out in the following.

The lowest state with 2 holes is a singlet:

$$|\psi\rangle = \cos\theta_2 \; |\tilde{\psi}\rangle - \sin\theta_2 \; |\tilde{\phi}\rangle \; , \qquad \tan 2\theta_2 = \frac{2\sqrt{2}\; V_0}{\Delta + 2J}, \tag{12}$$

where

$$|\tilde{\psi}\rangle = \frac{1}{\sqrt{2}} \; (d_\uparrow^{\dagger} c_\downarrow^{\dagger} - d_\downarrow^{\dagger} c_\uparrow^{\dagger}) \; |0\rangle \quad \text{and} \quad |\tilde{\phi}\rangle = c_\uparrow^{\dagger} c_\downarrow^{\dagger} \; |0\rangle \; .$$

The energy E_ψ of this singlet state,

$$E_\psi = -\frac{\Delta + 2J}{2} - \sqrt{\frac{(\Delta + 2J)^2}{4} + 2V_0^2} \; , \tag{13}$$

is separated by an energy of the order t^2/Δ (in the spin fluctuation regime $\Delta \gg t$), more exactly by

$$8\left(\frac{t^2}{\Delta} + \frac{t^2}{U-\Delta}\right)$$

from the energy E_τ of the triplet states. These are given by

$$|\tau_0\rangle = \frac{1}{\sqrt{2}} \; (d_\uparrow^{\dagger} c_\downarrow^{\dagger} + d_\downarrow^{\dagger} c_\uparrow^{\dagger}) \; |0\rangle, \quad |\tau_{2\sigma}\rangle = d_\sigma^{\dagger} c_\sigma^{\dagger} \; |0\rangle \tag{14}$$

with the energy

$$E_\tau = -\Delta \; . \tag{15}$$

The low-energy subspace of the two-hole-sector consists of these singlet (12) and triplet (14) states. It is separated by an energy of the order of Δ from the remaining doubly occupied oxygen state $|\tilde{\phi}\rangle$. In the following we will concentrate on the low-energy subspaces (10), (12), and (14) only.

Now, we will construct an effective Hamiltonian by projection of the hopping term (8) onto the low-energy subspace. But we have to distinguish if the hole creation operator changes the hole number from 1 to 2 or from 0 to 1. The first sector describes the singlet and triplet bands and will be derived first. The latter case corresponds to the lower occupied copper band and was not considered in Ref. 7.

C. Effective singlet-triplet problem

The projection on the relevant subspace in lowest order of $2t\lambda_1/\Delta$ is equivalent to the replacement of the oxygen- and copper-hole creation operators by[7]

$$c_\sigma^{\dagger} = 2\sigma A_c^{\psi} \; Y^{\psi\bar{\sigma}} + A_c^{\tau} \; Y^{\tau\bar{\sigma}} \; , \qquad X^{\sigma 0} = 2\sigma A_x^{\psi} \; Y^{\psi\bar{\sigma}} + A_x^{\tau} \; Y^{\tau\bar{\sigma}} \tag{16}$$

with $\sigma = \pm 1/2$ and

$$Y^{\psi\sigma} = |\psi\rangle\langle f_\sigma| \; , \qquad Y^{\tau\sigma} = \frac{1}{\sqrt{3}} \; |\tau_0\rangle\langle f_\sigma| + \sqrt{\frac{2}{3}} |\tau_{2\bar{\sigma}}\rangle\langle f_{\bar{\sigma}}| \; . \tag{17}$$

The parameters in (16) are given by

$$A_x^{\tau} = -\sqrt{\frac{3}{2}} \sin\theta_1 \quad , \quad A_x^{\psi} = -\frac{1}{\sqrt{2}} \sin\theta_1 \cos\theta_2,$$
$$A_c^{\tau} = -\sqrt{\frac{3}{2}} \cos\theta_1 \quad , \tag{18}$$
$$A_c^{\psi} = \sin\theta_1 \sin\theta_2 + \frac{1}{\sqrt{2}} \cos\theta_1 \cos\theta_2.$$

The new operators (17) are either a projection operator or the sum of two projection operators. Due to this similarity to the original Hubbard operators (4) we will denote these new operators as Hubbard operators as well. Note that they contain only transitions from the one-hole state (10) to the singlet and to the triplet states. The three triplet states are not independent from each other because they will be created only in the combination of $Y^{\tau\sigma}$. If we deal with each of the components of $Y^{\tau\sigma}$ separately we end up with a linear dependent system of equations of motion in the paramagnetic case. To avoid this, we present the further analysis in terms of the combined operator $Y^{\tau\sigma}$, which has been normalized in such a way that the resulting equation of motion (see Sec. IV) will occur in symmetrized form.

Now, if we put (16) into the hopping part of the Hamiltonian (8) we get the effective singlet-triplet Hamiltonian:

$$H = E_f \sum_{i,\sigma} Y_i^{\sigma\sigma} + E_\psi \sum_i Y_i^{\psi\psi} + E_\tau \sum_{i,\sigma} \frac{3}{2}\, Y_i^{\tau\sigma} Y_i^{\sigma\tau} + \sum_{i,j,\sigma}^{i\neq j} V_{ij}[K_{\psi\psi} Y_i^{\psi\sigma} Y_j^{\sigma\psi} - 2\sigma K_{\psi\tau}(Y_i^{\psi\sigma} Y_j^{\sigma\tau} + Y_j^{\tau\sigma} Y_i^{\sigma\psi}) + K_{\tau\tau} Y_i^{\tau\sigma} Y_j^{\sigma\tau}] \tag{19}$$

with $Y_i^{\sigma\sigma} = Y_i^{\sigma\psi} Y_i^{\psi\sigma}$ and $Y_i^{\psi\psi} = Y_i^{\psi\sigma} Y_i^{\sigma\psi}$ and with the following singlet-singlet, triplet-triplet, and singlet-triplet hopping parameters:

$$\begin{aligned} K_{\psi\psi} &= 2\tilde{A}_x^\psi A_c^\psi \quad , \quad \tilde{A}_x^\psi = A_x^\psi - \sqrt{2}\gamma \cos\theta_1 \cos\theta_2 \ , \\ K_{\tau\tau} &= 2A_x^\tau A_c^\tau \ , \\ K_{\psi\tau} &= \tilde{A}_x^\psi A_c^\tau + A_x^\tau A_c^\psi \ . \end{aligned} \tag{20}$$

Contrary to the previous derivation[7] of the singlet-triplet Hamiltonian (19), we chose another notation in terms of the combined triplet creation operator (17). If one neglects in (19) the triplet states and considers only the overlap to next neighbors then it corresponds to the hopping part of the t-J model.[1] In the limit $\Delta \gg t$ the effective hopping parameter $t_{\text{eff}} = V_1 K_{\psi\psi}$ goes over to the value found by Zhang and Rice, as was shown in Ref. 7. But in the intermediate region our method (which agrees with Ref. 8) gives much better values for t_{eff} than the original procedure. The exchange part of the t-J model was not derived here because we are not interested in the magnetic structure of the copper-oxide plane.

D. The copper band

Now we derive an effective Hamiltonian for the lower copperlike band which is occupied with holes. We need it for the comparison with results of our direct decoupling procedure.[13] We have to project the Hamiltonian (8) onto the low-energy subspace in the sector of transitions between hole-occupation 0 and 1. In that case the creation operators can be replaced by

$$c_\sigma^\dagger = -\sin\theta_1 \, Y^{\sigma 0}, \quad X^{\sigma 0} = \cos\theta_1 \, Y^{\sigma 0} \tag{21}$$

with

$$Y^{\sigma 0} = |f_\sigma\rangle\langle 0|$$

and correspondingly

$$Y^{\sigma\sigma} = |f_\sigma\rangle\langle f_\sigma| \ .$$

The replacement (21) gives simply the following effective problem (which was not derived in Ref. 7):

$$H = E_f \sum_{i,\sigma} Y_i^{\sigma\sigma} - \sum_{i,j,\sigma}^{i\neq j} V_{ij} \sin 2\theta_1 \, Y_i^{\sigma 0} Y_j^{0\sigma} \ . \tag{22}$$

We derived the effective problems for the singlet-triplet sector and for the copper band separately. These two sectors are separated by an energy of the order of Δ. Therefore, coupling effects between these two sectors are of second order in the small parameter $2t\lambda_1/\Delta$. These second-order contributions to the effective Hamiltonian were calculated in Ref. 7, but we neglect these effects in our first analysis of the singlet-triplet model.

III. TIME-REVERSAL SYMMETRY

The singlet-triplet mixing term in the effective Hamiltonian (19) depends explicitly on the spin σ. Nevertheless, the Hamiltonian (19) is invariant with respect to spin-reversal symmetry. That can be seen explicitly by taking into account that the operator of spin reversal K acts differently for the singlet and triplet operators:

$$K(Y_l^{\sigma\psi}) = -Y_l^{\bar{\sigma}\psi} \ , \tag{23}$$

but

$$K(Y_l^{\sigma\tau}) = Y_l^{\bar{\sigma}\tau}, \tag{24}$$

which is clear from the different definitions (12) and (14). Equations (23) and (24) can be considered as the definition of spin reversal within our effective problem (19).

There is yet another symmetry in our problem, namely, the symmetry with respect to complex conjugation. The operator of complex conjugation K_0 acts in the same way for singlet and triplet operators; for instance,

$$K_0(Y_l^{\sigma\psi}) = Y_l^{\psi\sigma} \ . \tag{25}$$

Both symmetries, spin reversal and complex conjugation, build the time reversal with the operator

$$T = K_0 K \ . \tag{26}$$

Because both symmetries are fulfilled independently within our singlet-triplet model, the time-reversal symmetry is fulfilled also. This symmetry simplifies the calculation considerably and gives rise to some restrictions of the final result. Therefore, it is worthwhile to investigate this symmetry in more detail. Let us discuss one important consequence of it.

We consider such a ground state, which does not break the spin-reversal symmetry (paramagnetic state). Then one can conclude from (23) and (24),

$$\langle Y_i^{\psi\sigma} Y_j^{\sigma\tau}\rangle = -\langle Y_i^{\psi\bar{\sigma}} Y_j^{\bar{\sigma}\tau}\rangle \ . \tag{27}$$

Furthermore, from the symmetry (25), it follows that the expectation value (27) is a real quantity. Due to the projection property of the Hubbard operators (17), the singlet-triplet transition amplitude (27) cannot depend on the spin σ for $i = j$. Therefore, this quantity must vanish at the same place:

$$\langle Y_i^{\psi\sigma} Y_i^{\sigma\tau}\rangle = 0 \ . \tag{28}$$

This could also be concluded because the singlet and the

triplet states represent the exact eigenstates within one elementary cell, and no local transitions between them are allowed. On the level of the effective Hamiltonian (19), however, it is a consequence of spin-reversal symmetry, or more generally a consequence of time-reversal symmetry.

IV. THE EQUATIONS OF MOTION FOR THE GF

The effective Hamiltonian (19) is a difficult problem due to the more complicated permutation relations for Hubbard operators. Therefore, one has to apply some approximations, which, perhaps, are not as justified as the model itself. The approximation by ordinary Fermi operators as in Ref. 6 neglects, in our opinion, very important effects of strong correlations. The projection technique[14–16] is more suitable for treating problems in terms of operators with unusual commutation relations. We explain now the method in the simplest approximation neglecting finite lifetime effects.

A. The projection method

We do not want to derive the formalism in a detailed way, but we give only the most important formulas for the special case of the singlet-triplet Hamiltonian (19). At first we have to choose the relevant basic operators. In our case these are the singlet and triplet creation operators $Y_i^{\psi\sigma}$ and $Y_i^{\tau\sigma}$. With these operators we build the susceptibility matrix

$$\chi_{\alpha\beta,ik} = \langle\{Y_i^{\sigma\alpha}, Y_k^{\beta\sigma}\}\rangle \ , \tag{29}$$

where $\{\cdots,\cdots\}$ denotes the anticommutator, $\langle\cdots\rangle$ the ground-state average, and the indices α and β are either ψ or τ. The susceptibility matrix and the frequency matrix,

$$\begin{aligned} \underline{\omega} &= \underline{\Omega}\underline{\chi}^{-1}, \\ \Omega_{\alpha\beta,ik} &= \langle\{[Y_i^{\sigma\alpha}, H], Y_k^{\beta\sigma}\}\rangle, \end{aligned} \tag{30}$$

determine the GF

$$G_{\alpha\beta,ik}(\omega) = -i\int_0^\infty dt\ e^{i(\omega+i0^+)t}\langle\{Y_i^{\sigma\alpha}(t), Y_k^{\beta\sigma}\}\rangle \tag{31}$$

by means of the matrix equation

$$(\omega + i0^+ - \underline{\omega})\underline{G} = \underline{\chi} \ . \tag{32}$$

Equation (32) represents only the first step in a hierarchy of equations of motion[15] and neglects, for instance, finite-lifetime effects altogether. However, it already displays some important effects of the strong correlation, as will be seen in the following consideration.

B. Susceptibility and frequency matrix

While calculating the matrix (30), higher-order correlation functions appear. They have to be approximated in a reasonable way. In the following, all higher-order correlation functions will be decoupled to such correlation functions, which can be calculated self-consistently. The decoupling of the spin-spin correlation function is consistent with the assumed classical paramagnetic ground state. We choose the number of holes h in the region $h \geq 1$, which corresponds to a slightly doped case. Then the singlet states should be partly occupied with holes. To simplify the resulting expressions one has to use the time-reversal symmetry mentioned in Sec. III. So one obtains for the susceptibility matrix

$$\begin{aligned} \underline{\chi}_{ik} &= \delta_{ik}\begin{pmatrix} \chi_\psi & 0 \\ 0 & \chi_\tau \end{pmatrix} , \\ \chi_\psi &= \langle Y_i^{\sigma\sigma}\rangle + \langle Y_i^{\psi\psi}\rangle \ , \\ \chi_\tau &= \frac{1}{3}\langle Y_i^{\sigma\sigma}\rangle + \frac{2}{3}\langle Y_i^{\bar\sigma\bar\sigma}\rangle + \langle Y_i^{\tau\sigma}Y_i^{\sigma\tau}\rangle \end{aligned} \tag{33}$$

and for the frequency matrix

$$\underline{\Omega}_{ik} = \delta_{ik}\begin{pmatrix} (E_\psi - E_f + \Delta E_\psi)\chi_\psi & 0 \\ 0 & (E_\tau - E_f + \Delta E_\tau)\chi_\tau \end{pmatrix} + (1-\delta_{ik})V_{ik}\begin{pmatrix} K_{\psi\psi}\chi_\psi^2 & (-2\sigma)K_{\psi\tau}\chi_\psi\chi_\tau \\ (-2\sigma)K_{\psi\tau}\chi_\psi\chi_\tau & K_{\tau\tau}\chi_\tau^2 \end{pmatrix} \ , \tag{34}$$

where

$$\begin{aligned} \Delta E_\psi &= \frac{1}{\chi_\psi}\frac{1}{N}\sum_{i,j}^{i\neq j} V_{ij}(K_{\psi\psi}M_{\psi\psi,ij} - K_{\tau\tau}M_{\tau\tau,ij}) \ , \\ \Delta E_\tau &= \frac{1}{\chi_\tau}\frac{1}{N}\sum_{i,j}^{i\neq j} V_{ij}\left(-\frac{3}{2}K_{\psi\psi}M_{\psi\psi,ij} + 2(2\sigma)K_{\psi\tau}M_{\psi\tau,ij} - \frac{1}{2}K_{\tau\tau}M_{\tau\tau,ij}\right) . \end{aligned} \tag{35}$$

The energy shifts (35) depend self-consistently on the singlet-triplet GF's itself by

$$M_{\alpha\beta,ij} = \langle Y_i^{\alpha\sigma}Y_j^{\sigma\beta}\rangle = -\frac{1}{\pi}\int_{-\infty}^{\mu} d\omega\ \mathrm{Im}\ G_{\beta\alpha,ji}(\omega) \tag{36}$$

with the chemical potential μ.

The doping dependence in (33) and (34) consists in a change in spectral weight (33) and the energy shifts (35). This will be discussed in detail in Sec. V B. In the undoped case ($h = 1$) one has

$$\chi_\psi = \chi_\tau = 1/2, \quad \Delta E_\psi = \Delta E_\tau = 0 \; . \tag{37}$$

The off-diagonal elements of (34) are proportional to the spin σ. This can be understood by using the spin-reversal symmetry (23) and (24), which acts differently for the diagonal and off-diagonal GF's,

$$G_{\psi\psi}(-\sigma) = G_{\psi\psi}(\sigma) \quad , \quad G_{\psi\tau}(-\sigma) = -G_{\psi\tau}(\sigma),$$

and for the $M_{\alpha\beta}$ (36) correspondingly. These relations are valid in the paramagnetic region.

To solve the equations of motion (32) we apply now the Fourier transformation to the frequency matrix:

$$\underline{\omega}(k) = \sum_m \underline{\omega}_{ll+m} e^{-ikm} \tag{38}$$

and to the susceptibility matrix (33). Using the definition (5) and the notation

$$\gamma_k = \tilde{\gamma}_k - 2\lambda_0 = 2 \sum_j^{l \neq j} \lambda_{lj} e^{ik(j-l)}, \tag{39}$$

we get the following equation of motion for the GF:

$$\left\{ \omega + i0^+ - \begin{pmatrix} A & \chi_\psi B \\ \chi_\tau B & C \end{pmatrix} \right\} \begin{pmatrix} G_{\psi\psi} & G_{\psi\tau} \\ G_{\psi\tau} & G_{\tau\tau} \end{pmatrix} = \begin{pmatrix} \chi_\psi & 0 \\ 0 & \chi_\tau \end{pmatrix} \; . \tag{40}$$

with the matrix elements

$$\begin{aligned} A &= E_\psi + \Delta E_\psi - E_f + \chi_\psi \; K_{\psi\psi} \; t \; \gamma_k \; , \\ B &= -K_{\psi\tau} \; t \; \gamma_k \; , \\ C &= E_\tau + \Delta E_\tau - E_f + \chi_\tau \; K_{\tau\tau} \; t \; \gamma_k \; . \end{aligned} \tag{41}$$

This 2×2 matrix can be solved very easily. The eigenvalues of (40) are the energies of the singlet and the triplet band

$$E_{T/S} = \frac{A+C}{2} \pm \sqrt{\frac{(A-C)^2}{4} + \chi_\psi \chi_\tau B^2} \; , \tag{42}$$

and the singlet and triplet GF's may be represented as

$$\begin{aligned} G_{\psi\psi} &= \frac{\chi_\psi}{\omega + i0^+ - E_S} \frac{E_S - C}{E_S - E_T} + \frac{\chi_\psi}{\omega + i0^+ - E_T} \frac{E_T - C}{E_T - E_S} \; , \\ G_{\tau\tau} &= \frac{\chi_\tau}{\omega + i0^+ - E_S} \frac{E_S - A}{E_S - E_T} + \frac{\chi_\tau}{\omega + i0^+ - E_T} \frac{E_T - A}{E_T - E_S} \; , \\ G_{\psi\tau} &= \frac{\chi_\psi \chi_\tau}{\omega + i0^+ - E_S} \frac{B}{E_S - E_T} + \frac{\chi_\psi \chi_\tau}{\omega + i0^+ - E_T} \frac{B}{E_T - E_S} \; . \end{aligned} \tag{43}$$

These GF's describe the singlet and the triplet band. They can be thought of being totally empty (for $h = 1$) or the singlet band is partly filled (for doping values $h > 1$).

C. The Green's function of the copper band

The application of the projection technique in this sector is much more easy. We choose the relevant operator $Y_i^{\sigma 0}$ and we obtain

$$\begin{aligned} \chi_{ik} &= \delta_{ik} \chi, \qquad \chi = \langle Y_i^{\sigma\sigma} \rangle \; , \\ \omega_{ik} &= \tilde{\omega}_{ik}/\chi = E_f \delta_{ik} - (1 - \delta_{ik}) \; V_{ik} \; \sin 2\theta_1 \; \chi \; . \end{aligned} \tag{44}$$

Here, the same approximations as above, i.e., the paramagnetic case and the neglect of antiferromagnetic correlations have been applied. The value of χ, which determines the spectral weight of the copper band, depends on the doping (see Sec. V B) and it is $1/2$ in the undoped case. To solve the equation of motion we use the Fourier transformation (38) and obtain from (44):

$$\omega(k) = E_f - \sin 2\theta_1 \; \chi \; t \; \gamma_k \; . \tag{45}$$

From (32), (44), and (45) one finds the GF of the lower band in the form

$$G(k) = \frac{\chi}{\omega + i0^+ - \omega(k)} \tag{46}$$

with $\omega(k)$ from (45). The only correlation effects in our simple approximation are the reduction of bandwidth and spectral strength of the lower band to one half of the original value. This implies already that in the half-filled case $h = 1$ the lower band is completely filled and we have a charge-transfer gap.

Now we will determine the number of relevant Fourier components for γ_k in the sum (39). We tested our procedure in the simple case of an uncorrelated tight-binding model, i.e., the problem (1) at $U = 0$. Then the exact dispersion of the lower band

$$E(k) = -\frac{\Delta}{2} - \sqrt{\frac{\Delta^2}{4} + t^2 \tilde{\gamma}_k^2} \tag{47}$$

with the $\tilde{\gamma}_k$ of (5) is very well known. The above-described procedure is applicable even at $U = 0$. For one hole one finds the same ground state (10) with the same energy (11). Projecting the hopping part onto the lower subspace (10) we obtain an effective Hamiltonian like (22). However, the lower band can be occupied with two holes, and thus we have to choose Fermi operators instead of Hubbard operators. The projected Hamiltonian can be simply diagonalized and gives a dispersion like (45) but with the full bandwidth ($\chi = 1$),

$$E(k) = E_f - \sin 2\theta_1 \; t \; \gamma_k \tag{48}$$

with the γ_k of (39). This corresponds to the Taylor expansion of (47) around E_f. In Fig. 1 we compare the exact result (47) with the approximation (48) taking into account in the sum (39) either all Fourier components [which restores $\tilde{\gamma}_k$ in the form (5)] or only the components λ_1 and λ_2. The consideration of all Fourier components is in favor only near to E_f but shows large deviations near $k = 0$, which is clear from the properties of the Taylor expansion. Therefore, in the following we will take

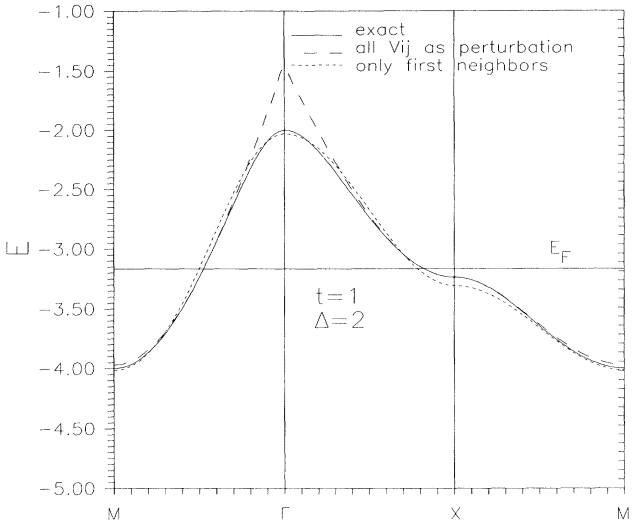

FIG. 1. Test of the Wannier expansion in the lower band of the uncorrelated case ($U = 0$, $\Delta = 2$, $t = 1$). Comparison of the exact dispersion relation with the Wannier expansion taking into account all or only the next (λ_1 and λ_2) expansion parameters. The points in k space are $M = (\pi, \pi), \Gamma = (0,0), X = (0,\pi)$.

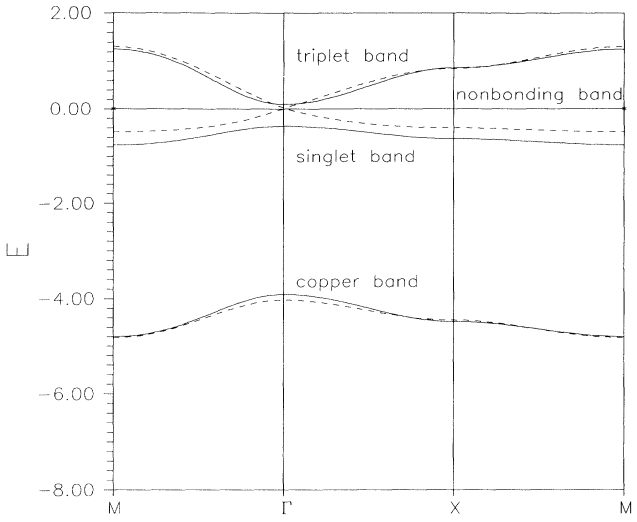

FIG. 2. Dispersion relation for $U = \infty$, $\Delta = 4$, $t = 1$ (full line) compared with the RPA result Ref. 13 (dashed line).

into account only λ_1 and λ_2, which display the overall shape of the band much better.

V. NUMERICAL RESULTS

A. Band structure and density of states

As already mentioned, the doping has no qualitative effects on the band structure in our procedure (because we fixed the magnetic structure). Only the spectral strength and the positions of the different bands change with doping. That will be discussed in the next section. Now we present the results for $h = 1$.

Let us first discuss the band structure calculated from the poles of (43) and (46). That is the singlet, the triplet (42), and the copper bands (45). In Fig. 2 we show the results for $U = \infty, \Delta = 4, t = 1$ and compare them with our former RPA procedure.[13] In that case the parameters of the effective singlet-triplet Hamiltonian (19) are $E_f = -4.77$, $E_\psi - E_f = -0.6$, $K_{\psi\psi} = -0.355$, $K_{\tau\tau} = 1.038$, $K_{\psi\tau} = -0.077$.[7] The negative sign of $K_{\psi\psi}$ guarantees that the singlet band has qualitatively the same dispersion as the copper band. Only the singlet bandwidth is reduced compared with the copper bandwidth. In the doped case $h > 1$ one finds the Fermi level within the singlet band.

The ordinary band-structure calculations[17] interpret the spectroscopic data[18,19] as if the Fermi level is located in the antibonding (in the electron picture) copperlike band. This can be justified by the similarity of the dispersion and the Fermi surface shape in spectroscopic measurements and theoretical calculations.[17] The only difference is that the experimental value of the bandwidth of the band crossing the Fermi surface is smaller in comparison with the theoretical one. In our calculation we found the same dispersion for the singlet and the copper band. This allows us to propose another interpretation of the spectroscopic data with the Fermi level situated in the singlet band.

Such a band as the singlet band in our calculation has also been obtained starting from the antiferromagnetic ground state in Ref. 12 or within the paramagnetic case as in Refs. 11 and 13. In the present analysis the singlet band already exists in the extremely small doping region. This is in agreement with Refs. 12 and 13 but in contrast with the results of Matsumoto, Sasaki, and Tachiki.[11] There, the singlet band arises only with increasing doping, which seems to be due to their special decoupling procedure.

To check our results we compared them with our former results.[13] In Ref. 13 we applied a GF-decoupling scheme to the Hamiltonian (3) in the limit $U \to \infty$. We introduced the singlet operator $p_{i\sigma}^{(s)\dagger} - p_{i\bar{\sigma}}^{(s)\dagger} X_i^{\sigma\bar{\sigma}}$ additionally to the copper and oxygen creation operators $X_i^{\sigma 0}$ and $p_{i\sigma}^{(s)\dagger}$ and decoupled the problem in a RPA-like manner.[13] Thus, we reached a reasonable description of the singlet band. The agreement of our present results with the RPA procedure is rather good, especially for the copper and the triplet band. Only the singlet band does not appear at the correct place in the RPA, namely, it is shifted to higher values of the energy.

Next we calculated the density of states. For that we had to transform the singlet and triplet GF's (40) back to the original copper G_{DD} and oxygen GF's G_{PP}. With (16) we obtain

$$G_{PP} = 2(A_c^\psi)^2 G_{\psi\psi} + 2(A_c^\tau)^2 G_{\tau\tau} + 4(A_c^\psi A_c^\tau) G_{\psi\tau} \,, \tag{49}$$

$$G_{DD} = 2(A_x^\psi)^2 G_{\psi\psi} + 2(A_x^\tau)^2 G_{\tau\tau} + 4(A_x^\psi A_x^\tau) G_{\psi\tau}$$

in the singlet-triplet sector. For brevity we introduce the notation

$$G_{PP} + G_{DD} = C_{\psi\psi} G_{\psi\psi} + C_{\tau\tau} G_{\tau\tau} + C_{\psi\tau} G_{\psi\tau}. \tag{50}$$

For the lower band one has simply, from (21),

$$G_{PP} = 2\sin^2\theta_1 G, \qquad G_{DD} = 2\cos^2\theta_1 G\ . \tag{51}$$

To obtain the density of states we use (49) and (43) and carry out the k sums with the help of a two-dimensional analogy of the tetraeder method.[20] The result is shown in Fig. 3.

One can also calculate the spectral strength of every band. From (43) and (49) one finds the spectral strength of the triplet band

$$O_T = -\frac{1}{\pi}\int_{\omega_{tu}}^{\omega_{to}} \frac{1}{N}\sum_k \mathrm{Im}\,(G_{PP} + G_{DD})\, d\omega = C_{\tau\tau}\,\chi_\tau \tag{52}$$

and of the singlet band

$$O_S = -\frac{1}{\pi}\int_{\omega_{su}}^{\omega_{so}} \frac{1}{N}\sum_k \mathrm{Im}\,(G_{PP}+G_{DD})\, d\omega = C_{\psi\psi}\,\chi_\psi, \tag{53}$$

where ω_{tu}, ω_{to} and ω_{su}, ω_{so} denote the band edges of the triplet and of the singlet band. In the undoped case ($h = 1$) of Fig. 3 these values are $O_T = 1.5$ and $O_S = 0.62$. Please note that, in contrast with O_T, the value of O_S at $h = 1$ depends on the parameters. It approaches 1/2 in the limit $U = \infty$, $\Delta \gg t$. The reason for this difference is not well understood.

The spectral strength of the copper band can be computed from (46) and (51):

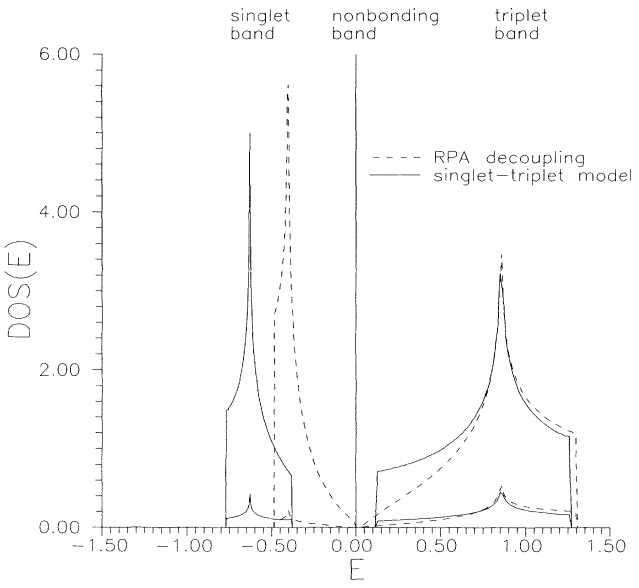

FIG. 3. The total and the copper density of states for $U = \infty$, $\Delta = 4$, $t = 1$ compared with the RPA result. Note that the spectral weights of the singlet and the triplet bands are 0.62 and 1.5, respectively.

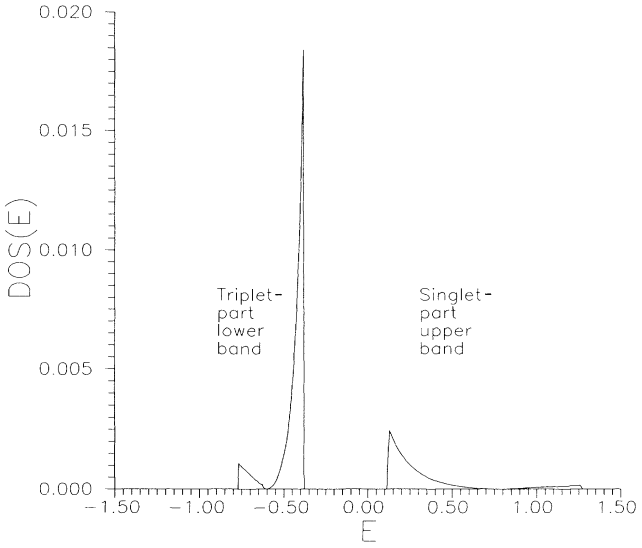

FIG. 4. Triplet part in the singlet band and vice versa for the parameter values of Fig. 3.

$$O_{\mathrm{Cu}} = 2\,(\cos^2\theta_1 + \sin^2\theta_1)\,\chi = 2\,\chi \tag{54}$$

and it is unity in the undoped case, as it should be. The spectral weights O_T, O_S, and O_{Cu} depend on the doping as will be discussed later (Fig. 5).

It is seen very clearly from Fig. 3 that both methods give a singlet band of predominantly oxygen character in agreement with Ref. 9. And also the results for the spectral strength agree more or less.

Next, in Fig. 4 we show the triplet part $\sim$ Im $G_{\tau\tau}$ of the singlet band and vice versa. This contribution is very small (please note the different scale in Fig. 4). The triplet contribution is only one fifth of a percent of the total weight of the singlet band. This small contribution is due to the small value of $K_{\psi\tau}$. Furthermore, the contribution vanishes exactly in the middle of the band. This is because the local singlet-triplet coupling is forbidden (28) due to the time-reversal symmetry as mentioned above. The mixed GF $G_{\psi\tau}$ changes its sign in the middle of the band, and due to (28) it fulfills the sum rule

$$\sum_k \mathrm{Im}\; G_{\psi\tau}(k) = 0 \tag{55}$$

in every band separately.

B. Influence of doping

Last, we discuss the results of a self-consistent solution for finite doping ($1 < h < 2$) with the chemical potential μ in the singlet band. The formulas to determine the energy shifts ΔE_ψ and ΔE_τ are already given in (35). To determine also the change in χ_ψ and χ_τ (33), we must note that $\langle Y_i^{\sigma\sigma} + Y_i^{\bar\sigma\bar\sigma}\rangle$ is the density of elementary cells, which are occupied with exactly one hole. This density decreases with increasing doping values. In our simple procedure (without coupling between the one- and the two-hole sector) it is given as

$$\chi = \langle Y_i^{\sigma\sigma} \rangle = 1 - \frac{h}{2} \,. \tag{56}$$

The density of holes can be calculated from

$$h = -\frac{1}{\pi} \int_{-\infty}^{\mu} d\omega \, \frac{1}{N} \sum_k \mathrm{Im} \, (G_{PP} + G_{DD}), \tag{57}$$

which has a contribution from the one-hole sector (51) and from the two-hole sector (50),

$$h = 2\,\chi + C_{\psi\psi}\,\chi_\psi\,S_\psi + C_{\tau\tau}\,\chi_\tau\,S_\tau + C_{\psi\tau}\,\chi_\psi\,\chi_\tau\,S_{\psi\tau}\,, \tag{58}$$

where the following sums over the occupied k values have been defined

$$S_\psi = \frac{1}{N} \sum_k^{\mathrm{occ}} \frac{E_S - C}{E_S - E_T}, \qquad S_\tau = \frac{1}{N} \sum_k^{\mathrm{occ}} \frac{E_S - A}{E_S - E_T},$$

and

$$S_{\psi\tau} = \frac{1}{N} \sum_k^{\mathrm{occ}} \frac{B}{E_S - E_T} \,. \tag{59}$$

From (56) and (58) one finds

$$h = 1 + \frac{1}{2} \, (C_{\psi\psi}\,\chi_\psi\,S_\psi + C_{\tau\tau}\,\chi_\tau\,S_\tau + C_{\psi\tau}\,\chi_\psi\,\chi_\tau\,S_{\psi\tau}) \,. \tag{60}$$

Using the expression (60) in (33), which also can be written as

$$\begin{aligned} \chi_\psi &= 1 - \frac{h}{2} + \chi_\psi\,S_\psi \,, \\ \chi_\tau &= 1 - \frac{h}{2} + \chi_\tau\,S_\tau \,, \end{aligned} \tag{61}$$

one obtains two coupled equations to determine χ_ψ and χ_τ. Their solution is

$$\chi_\psi = \frac{\tilde{\chi}}{1 - S_\psi} \quad \text{and} \quad \chi_\tau = \frac{\tilde{\chi}}{1 - S_\tau} \tag{62}$$

with

$$\tilde{\chi} = -\frac{b}{2a} + \sqrt{\frac{b^2}{4a^2} - \frac{c}{a}}$$

and

$$\begin{aligned} a &= S_{\psi\tau}\frac{C_{\psi\tau}}{4} \,, \\ b &= (1 - S_\psi)(1 - S_\tau) + (1 - S_\psi)S_\tau\frac{C_{\tau\tau}}{4} \\ &\quad + (1 - S_\tau)S_\psi\frac{C_{\psi\psi}}{4} \,, \\ c &= -\frac{1}{2}(1 - S_\psi)(1 - S_\tau) \,. \end{aligned} \tag{63}$$

For a numerical solution we fix the number of occupied k values, and determine in every step the energy shifts ΔE_ψ and ΔE_τ from (35), as well as χ_ψ and χ_τ from (62), using the sums (59) until we reach self-consistency. The doping dependence of the spectral strength O_S, O_T, and O_{Cu} (52)–(54) is given in Fig. 5. For illustration we show also the fraction $F = N_k/N$ of occupied k values N_k.

In the undoped case the spectral strength of the singlet band is 0.62. But one expects that the singlet band can be filled up to $h = 2$, since one can replace $|f_\sigma\rangle$ by $|\psi\rangle$ at each site. Therefore, the spectral strength of the singlet band should increase with doping. Due to a sum rule the spectral weights of the copper and the triplet bands should decrease. Our results in Fig. 5 display this expected behavior very nicely. Such a transfer of spectral weight has also been found in spectroscopic measurements[21] and in exact diagonalization studies.[22–24] Eskes, Meinders, and Sawatzky[22] took this transfer of spectral weight as a sign of strong correlation. They plotted the integrated spectral weight of the singlet band up to the chemical potential $C_{\psi\psi}\chi_\psi S_\psi$ versus the doping $h - 1$ and found a proportionality factor $\alpha = 2$ only for large enough t_{pd}. We find here in any case $\alpha = 2$, since we neglected the direct oxygen-oxygen hopping t_{pp}.

One also can see from Fig. 5 that the filling of the singlet band occurs in an asymmetric way and that it is already half filled ($F = 0.5$) for $h = 1.24$. Only for that special doping value the original Fermi surface from ordinary band-structure calculations will be recovered. We think that the strong dependence of the Fermi surface on doping is a drawback of our method. It is in contradiction to experimental results[18,19] and to the Luttinger theorem. Let us note, for comparison, that the slave boson calculations[25,26] or the similar Gutzwiller approximation[27] fulfill the Luttinger theorem. However, on the other hand, they cannot display any transfer of spectral weight. Perhaps in the present approach the Fermi surface can be fixed if we calculate the lifetime of the quasiparticles.

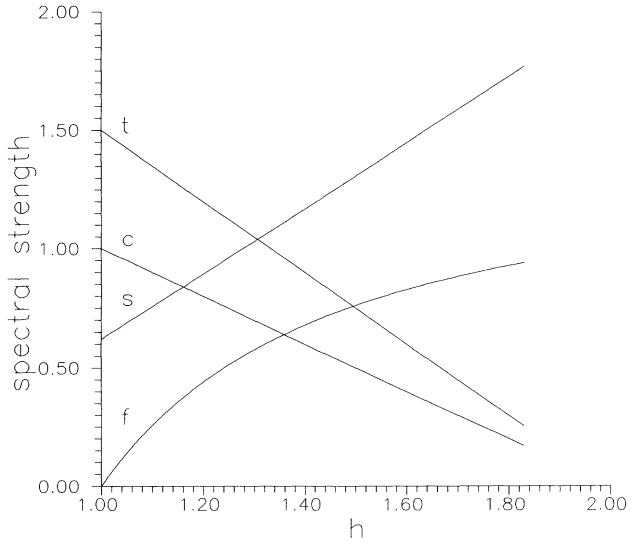

FIG. 5. Doping dependence of the spectral weights of the copper (c), singlet (s) and triplet (t) bands. The parameter values are $U = \infty$, $\Delta = 4$, $t = 1$ and the fraction F of occupied k values in the singlet band is also shown (f).

The other shortcoming of our analysis is the neglect of antiferromagnetic correlations. The spin background is expected to have a large influence on the electronic structure. Indeed, the analysis of the one-hole-motion in the antiferromagnetic state[28] gives another dispersion than we found. It is determined by next-nearest-neighbor hopping rather than the nearest-neighbor hopping, in our case. But we expect that at moderate doping values the character of the dispersion changes to the nearest-neighbor hopping. This was shown by the diagonalization of small clusters.[29] Our present method also cannot divide the coherent from the incoherent part of the spectrum, which is quite important.[28,29] But the momentum sum of the spectral function (with contributions from both parts of the spectrum) is roughly the same if one starts from the AFM background as in Ref. 12, or if one considers our results in the paramagnetic case.

VI. CONCLUSION

We analyzed the recently derived singlet-triplet model in the paramagnetic case. This effective model is an extension of the Zhang-Rice procedure to the charge-fluctuation regime, also including the triplet states. We developed these ideas up to a detailed calculation of the band structure and the density of states. The general idea of the procedure, i.e., the exact diagonalization of a small cluster and the consideration of the hopping term such as a perturbation, while projecting out some higher states, seems worthwhile to also try on other problems. It has been shown that the projection technique is a very convenient way to derive the equations of motion for difficult effective problems in terms of Hubbard operators. The numerical results show that the Fermi level is situated in the singlet band, which is mainly of oxygen character and has the same dispersion as the copper band. The spectral strength of every band was calculated and a transfer of spectral weight has been found with doping. This seems to be in agreement with some experiments in the doped, paramagnetic region. The mixing between singlet and triplet bands has been found to be very small. This is a further argument for the validity of the t-J model. On the other hand, our procedure gives us the possibility to study in a systematic way the relation between the two models and to investigate some minor effects of the singlet-triplet coupling. This was shown here for the density of states.

ACKNOWLEDGMENTS

We thank Uwe Thiele for assistance in the numerical calculations. One of the authors (R.H.) thanks Professor K. Becker and Professor P. Fulde for useful discussions.

[1]F.C. Zhang and T.M. Rice, Phys. Rev. B **37**, 3759 (1988).
[2]V.J. Emery, Phys. Rev. Lett. **58**, 2795 (1987).
[3]V.J. Emery and G. Reiter, Phys. Rev. B **38**, 11 938 (1988).
[4]F.C. Zhang and T.M. Rice, Phys. Rev. B **41**, 7243 (1990).
[5]V.J. Emery and G. Reiter, Phys. Rev. B **41**, 7247 (1990).
[6]H.P. Bang, T. Xiang, Z.B. Su, and L. Yu, Phys. Rev. B **41**, 7209 (1990).
[7]S.V. Lovtsov and V.Yu. Yushankhai, Physica C **179**, 159 (1991).
[8]J.H. Jefferson, H. Eskes, and L.F. Feiner, Phys. Rev. B **45**, 7959 (1992); J.H. Jefferson, Physica B **165&166**, 1013 (1990).
[9]N. Nücker, J. Fink, J.C. Fuggle, P.J. Durham, and W.M. Temmermann, Phys. Rev. B **37**, 5158 (1988).
[10]H. Romberg, M. Alexander, N. Nücker, P. Adelmann, and J. Fink, Phys. Rev. B **42**, 8768 (1990).
[11]H. Matsumoto, M. Sasaki, and M. Tachiki, Solid State Commun. **71**, 829 (1989).
[12]K.W. Becker, W. Brenig, and P. Fulde, Z. Phys. B **81**, 165 (1990).
[13]R. Hayn, Z. Phys. B **85**, 169 (1991).
[14]N.M. Plakida, V.Yu. Yushankhai, and I.V. Stasyuk, Physica C **160**, 80 (1989).
[15]Yu.A. Tserkovnikov, Theor. Matem. Fiz. **49**, 219 (1981) (in Russian).
[16]R. Hayn and V. Yushankhai, Phys. Status Solidi B **166**, 415 (1991).
[17]W.E. Pickett, Rev. Mod. Phys. **61**, 433 (1989).
[18]H.J. Bernhoff, K. Tsushima, and J.M. Nicholls, Europhys. Lett. **13**, 537 (1990).
[19]G. Mante, R. Claessen, T. Buslaps, S. Harm, R. Manzke, M. Skibowski, and J. Fink, Z. Phys. B **80**, 181 (1990).
[20]P. Ziesche and G. Lehmann, *Ergebnisse in der Elektronentheorie der Metalle* (Akademie-Verlag, Berlin, 1983), p. 543.
[21]C.T. Chen *et al.*, Phys. Rev. Lett. **66**, 104 (1991).
[22]H. Eskes, M.B.J. Meinders, and G.A. Sawatzky, Phys. Rev. Lett. **67**, 1035 (1991).
[23]P. Horsch and W. Stephan in *Dynamics of Magnetic Fluctuations in High Temperature Superconductors*, Proceedings of the NATO Advanced Research Workshop, edited by G. Reiter, P. Horsch, and G. Psaltakis (Plenum, New York, 1991).
[24]T. Tohyama and S. Maekawa, Physica C **191**, 193 (1992).
[25]G. Kotliar, P.A. Lee, and N. Read, Physica C **153-155**, 538 (1988).
[26]C.A. Balseiro, M. Avignon, A.G. Rojo, and B. Alascio, Phys. Rev. Lett. **62**, 2624 (1989).
[27]R. Hayn and R. Schumann, Physica C **174**, 199 (1991).
[28]K.J. von Szczepanski, P. Horsch, W. Stephan, and M. Ziegler, Phys. Rev. B **41**, 2017 (1990).
[29]W. Stephan and P. Horsch, Phys. Rev. Lett. **66**, 2258 (1991).